International Conference
Nuclear Energy for New Europe 2003
Portorož, Slovenia, September 8-11, 2003
http://www.drustvo-js.si/port2003

Fluid Induced Structural Vibrations in Steam Generators and Heat Exchangers

Ivan Catton, Pierangelo Adinolfi, Omar Alquaddoomi
Department of Mechanical and Aerospace Engineering
University of California, Los Angeles
Los Angeles, CA 90095-1597, United States
catton@ucla.edu

ABSTRACT

Fluid-elastic instability (FEI) in tube bundle heat exchangers was studied experimentally. The motion of an array of 15 stainless steel vibrating tubes (∅ 25.4mm) in water cross-flow, suspended using stainless steel piano wire has been recorded with a CCD camera. The individual motion and relative motion of the tubes are reported and can be used for computational model validation. The relative displacement of the tubes allows identification of the most potentially damaging patterns of tube bundle vibration. A critical reduced velocity may be determined by specification of an allowable limit on tube motion amplitude. Measurements were made for various tube array configurations, tube natural frequencies and flow conditions.

1 INTRODUCTION

The importance of heat exchangers to the process industry is well known and are one of the most numerous pieces of equipment found. Their design is a balance between trying to optimize the heat transfer characteristics and trying to avoid flow-induced vibrations that will cause premature wear or damage to the device. Flow-induced vibration is an extremely important phenomenon that has led to numerous failures in heat exchanger equipment. It has been a major cause of concern in the nuclear industry for several decades. Many incidents of failure of heat exchangers due to apparent flow-induced vibration have been reported through the USNRC incident reporting system. Almost all heat exchangers have to deal with this problem during their operation. The phenomenon has been studied since the 1970s and the database of experimental studies on flow-induced vibration is constantly updated with new findings and improved design criteria for heat exchangers. Flow-induced vibration is not limited to nuclear power plants, but to any type of heat exchanger used in various industrial applications such as chemical processing, or refrigeration and air conditioning. Specifically, shell-and-tube type heat exchangers experience flow-induced vibration due to the high velocity flow over the tube banks. Flow-induced vibration in these heat exchangers leads to equipment breakdown and, hence, expensive repair and process shutdown. The resulting vibration mode is often referred to as fluid-elastic instability [1,2]. This phenomenon, while not the only source of flow induced vibration, is the more dangerous type present in heat exchanger operations, contributing to fretting wear and eventual mechanical failure.

A part of this study led to the development of the tools necessary for a comprehensive investigation of fluid-elastic instability in tube bundles, including the sensitivity of the mechanism to various geometrical and physical parameters of the system, to be made. It is

hoped that complete data sets from such experiments will lead to improved design of tube-bundle type heat exchangers susceptible to FEI. In order to achieve this goal, an array of simply supported tubes is subjected to water cross-flow and observed using a novel approach. The absolute displacements of each tube, and the displacement of each tube relative to the others, have been recorded using a real-time imaging process. The images are analyzed to extract the two-dimensional vibration of the array and, hence, to determine instability maps for a specified tube array configuration. Our earlier publications, see [3,4] focused on the development and use of the experimental method and will only be summarized here.

Experimental measurements of frequencies and amplitudes of FEI induced vibration are most often for a single flexible tube within a tube bundle and most often inferred from strain guage readings or integrated accelerometer data. The image data acquired at these reduced velocities are direct and clearly exhibit the large amplitude vibrations characteristic of the fluid-elastic instability. The results were surprising and exhibited behaviour not reported elsewhere.

A summary of past work and some design guidance was given by Pettigrew and Taylor [5]. The results obtained in this work seem reasonable when compared with other reported values for the FEI onset [5] under similar conditions, providing some degree of validation for the measurement methods. This validation is of primary importance because the ability to correctly and accurately predict the onset of FEI for a well-known configuration is a mandatory check, required before any application of the methodology to more complex situations or measurements.

2 EXPERIMENTAL SETUP

The experimental apparatus includes a flow loop consisting of four main parts: a reservoir, a pump, a surge tank and the test section (Fig.1). A 15hp (11kW) centrifugal pump provides the pressure to drive the fluid flow throughout the loop. Downstream from the surge tank, the fluid enters the test section; an in-line differential pressure flow meter (∅ 2" (5.1cm)) is installed to observe the flow rate. The flow meter can measure flow velocities between 0 and 350 GPM (22 dm^3/s) to within ± 0.075% of the calibrated span. The water necessary to run the experiment is stored in the main water tank. The test section (Fig.2) consists of two stainless steel diffusers separated by an acrylic main box where the tubes, the objects of the measurements, are located. At the end of the angled part of the upstream diffuser there is a straight section which houses an aluminum honeycomb structure, 3 inches (7.6cm) in cell depth, to straighten the incoming flow.

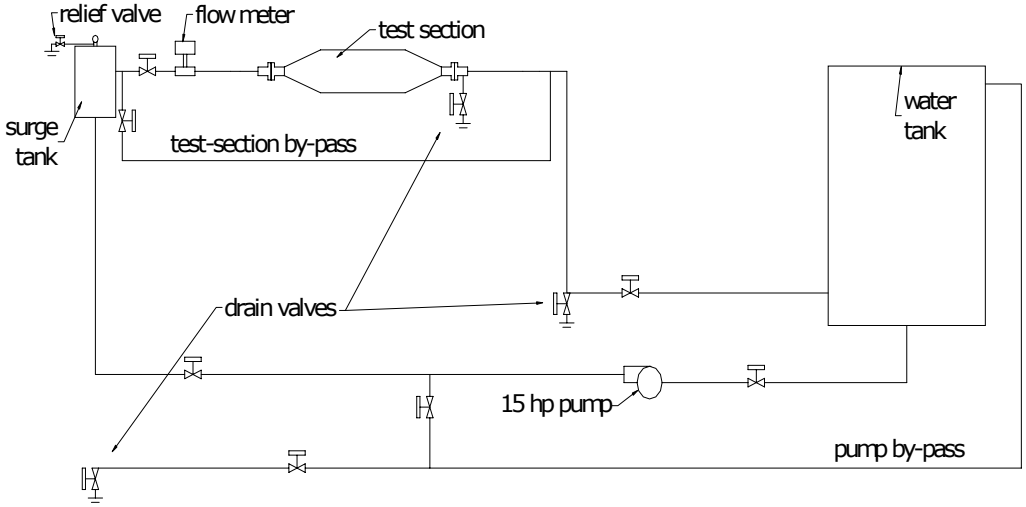

Figure 1. Schematic of the flow loop

The external dimensions of the acrylic box are 16 inches in length, 6.6 inches in height and 10.25 inches wide. It is possible to identify two main parts. In the first part, a 3 x 5 square array of plain fixed acrylic tubes and 10 acrylic half-tubes are fitted in the box. The function of these fixed tubes is to develop the flow upstream of the vibrating tubes such that the vibrating tubes are subject to an oscillatory flow and not a uniform flow, which is hoped to more closely model the situation in heat exchangers. In the second part, a 3 x 5 square array of stainless steel tubes, suspended by piano wire, constitute the vibrating tubes. These tubes are free both to vibrate linearly in the plane perpendicular to their axes, and to rotate about their axes. The vibrating tubes are the components for the actual heat exchanger model, and are thus the focus of the experimental observations. The stainless steel tubes are 1-inch diameter and 9 inches long. To assemble the tubes, a clearance of 1/8" is provided between each tube end and the ½ inch thick side panels.

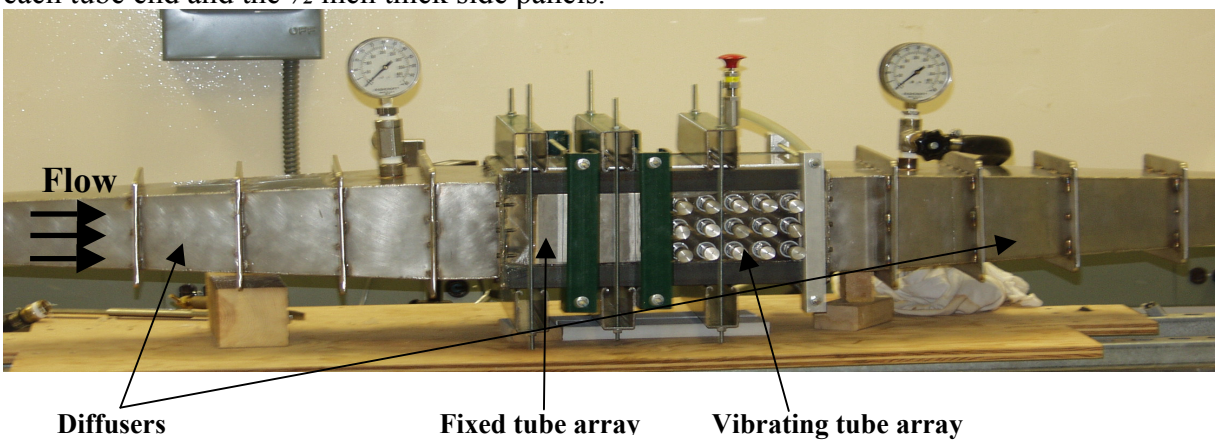

Figure 2. Test section

The inside bore of each vibrating tube is threaded and two quarter inch thick disks are inserted by equal distances at each end. The disks provide fixed-point anchors for the piano wires, which are inserted through small clearance holes and fixed on the interior of the disks with an epoxy resin. The remaining end of one of the piano wires goes through a custom-made stainless steel insert screwed into the acrylic wall. This insert is designed to hold the wire with a setscrew device. On the other side, the wire passes through another customized insert and is held by a cap placed on the top of a precision compression spring. The spring can be relaxed or compressed in order to change the tension of the wire. In this way it is possible to control the natural frequency of the suspended tube, as illustrated in Fig. 3.

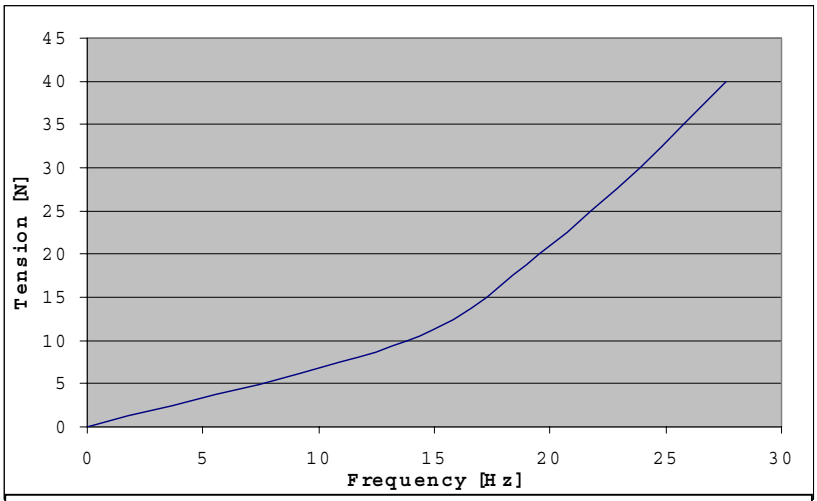

Figure 3. Relationship between tension of the wire and natural frequency of the tube

A complete detailed description of the experimental apparatus and its operation can be found in [4].

2.1 Data Acquisition

Using two high-speed digital cameras, sequential images of the tube array are captured for a period of vibration during which the tubes are excited by the water cross-flow at a specific velocity. Sets of these "raw" (i.e. unprocessed) images, captured at a high time frequency, are basically movies of the tube motion at different flow speeds: one movie, equal to one thousand images (or about 8 seconds), is recorded for a specified mean flow speed. After some processing and analysis, the resulting data allows for the detailed inspection of the tube array vibration, in addition to the average vibration magnitude for a specified steady flow condition (i.e. for each flow speed). The cameras are CCD type sensors with a spatial resolution of 640 by 480 pixels and capture images at a rate of 120 frames per second.

2.2 Image Processing & Analysis s

Image extraction and pre-processing has been automated and can be run as a batch process once a tube ROI (Region of Interest) within a particular set of raw images has been identified. The method can be applied to each of the visible vibrating tubes within each of the full raw images from the different time series. The result is a set of smaller binary images containing the profile of the respective tube of interest. Sets of these small images can be differentiated by both the position of the tube within the array, and by the flow velocity during which the image series was recorded. The binary ROI images are automatically analyzed using either or both of two analysis programs.

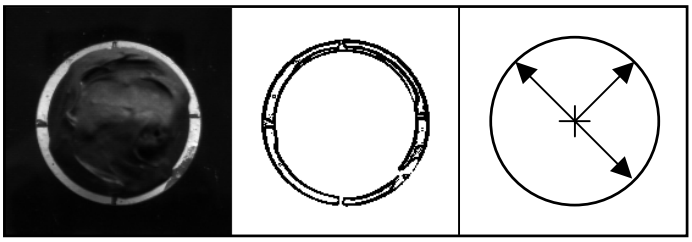

Figure 4. Left: the raw extracted ROI image of the tube profile; Center: binary tube image (after processing); Right: schematic of the circular interpolation using 3 perimeter points from the center image.

Figure 4 illustrates the images at the various stages in the processing and analysis routine. The left image is an ROI image of the center tube, extracted from the raw array image. The center image is the result of the image pre-processing and the left image is a representation of the tube location analysis using the 3-point interpolation method. This method and the cross-correlation analysis method are described in [3,4]. The center position of each tube in the array, for each frame (i.e. for all times in the movie interval), relative to the equilibrium position, is recorded. The equilibrium position of a tube refers to the center coordinates of the tube with no flow-induced displacement, i.e. the position of the suspended tube in still water. These equilibrium positions are determined using the images recorded at the (initial) zero flow rate. The Euclidean distance between the instantaneous tube center coordinates (during induced vibration) and the equilibrium position of a specific tube is referred to as the *absolute* displacement of the tube.

It was observed from early experiments that the displacement due to hydrodynamic drag of a tube subject to the water cross-flow is a significant component of the absolute displacement magnitude. This displacement is approximately constant in time when averaged over a time interval significantly longer than the period obtained by dividing the characteristic length of the flow by the flow speed (in this case, the diameter of a tube divided by the maximum gap velocity). Using the total time of the movie as a basis, the time-averaged absolute displacement is calculated and referred to as the *static* or *drag* displacement. Subtraction of this static displacement from the absolute displacement gives us the definition for the *dynamic* displacement: the displacement of the tube about the average position of the

tube during some time interval, at a fixed mean flow velocity. The dynamic displacement is the component of motion that is identified with the actual vibration of the tube, that is, the time-varying oscillatory component of the tube motion.

3 RESULTS

3.1 Rectangular Array

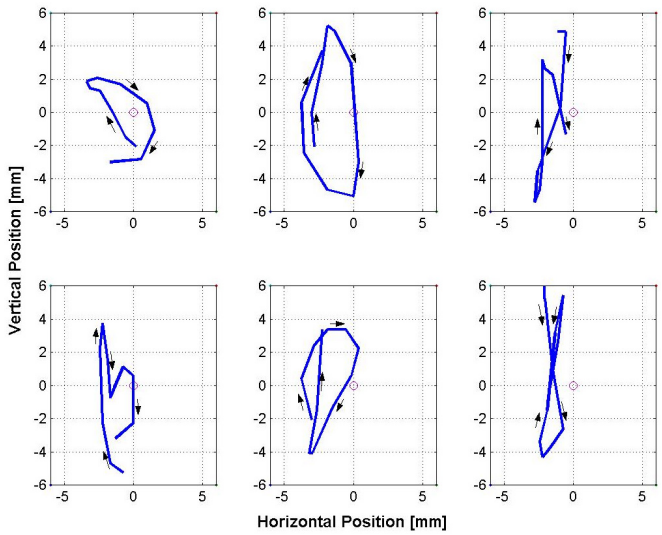

Figure 5. Pathlines of the center tube coordinates over six sequential 0.1-second time intervals during the instability. Arrows indicate the direction of motion of the tube and the red circle indicates the equilibrium position. The flow is from right to left.

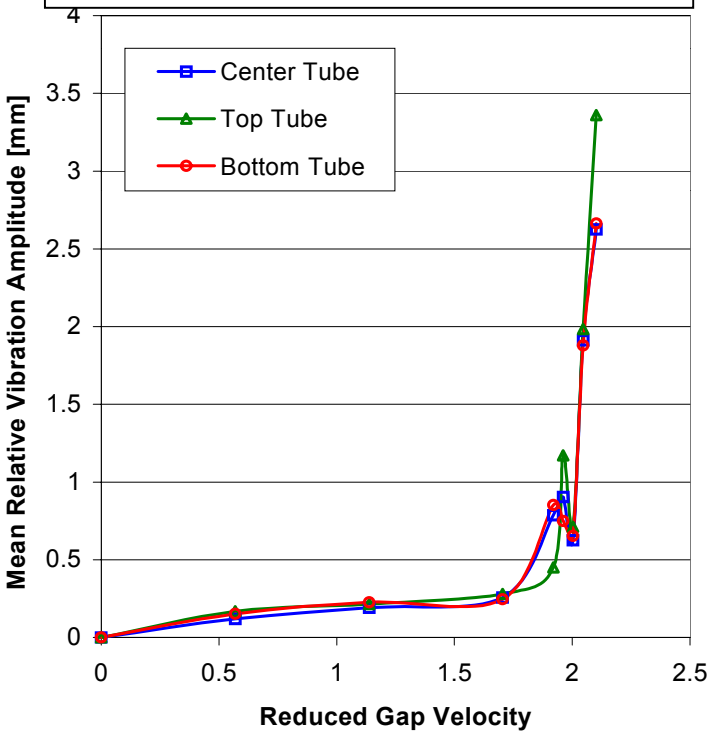

Figure 6. Instability map for three tubes of a square array with pitch-to-diameter ratio of 1.4

The distribution of the tube position coordinates also shows that the tube vibrates in a more or less random fashion; the tube position seems to be distributed evenly about the static displacement point for the data taken so far. This indicates that the forcing on the tube is isotropic under the test conditions. This may not be true over a larger range of reduced velocities or for different tube array configurations; further testing must be done to gain an understanding of the tube orbits. Fig. 5 shows some orbits of the center tube. It can be seen that the tube is driven in a generally clockwise orbit, but also experiences several sudden changes in direction, with particular preference to the vertical direction. The plot of a single tube provides information of limited interest towards investigation of the tube array dynamics, but is given here as an example of the capability of the methods to capture the instantaneous structural motions.

A second measure of importance is the average magnitude of the tube vibration or, equivalently, the average dynamic displacement of the tubes over a range of reduced velocities. This measure is plotted in Fig 6. The data trends both show a gradual increase in the average vibration amplitude with increasing reduced velocity, as expected. A sudden and violent increase in the vibration is indicative of the onset of the fluid-elastic instability and is predicted by both the correlation and interpolation methods to occur at a critical

velocity of approximately two. The image data acquired at these reduced velocities clearly exhibits the large amplitude vibrations characteristic of the fluid-elastic instability. These results seem reasonable when compared with other reported values for the FEI onset [5] under similar conditions, providing some degree of validation for the measurement methods. This validation is of primary importance because the ability to correctly and accurately predict the onset of FEI for a well-known configuration is a mandatory check, required before any application of the methodology to more complex situations or measurements.

It is can also be seen that a very slight, but distinct jump in the vibration amplitude occurs directly before the critical velocity. This "hump" is typically attributed to vortex shedding. The Strouhal number, defined as

$$S = \frac{f_s D}{U_p} \tag{1}$$

may be calculated once the vortex shedding frequency, corresponding to the reduced velocity at which the resonance occurs, is measured [1]. The Fourier transforms of the time varying horizontal and vertical tube position functions were evaluated for the data at this reduced velocity, providing the tube structural frequency of vibration in both of the principal directions of motion. The vortex shedding frequency is then approximated by taking the average of these two structural vibration frequencies, and the Strouhal number is directly computed by Eq. (1). Using the information processed thus far, the Strouhal number was determined to vary between 0.4 and 0.5.

Additionally, a few qualitative aspects of the fluid-elastic instability have been noted. The onset of the instability occurred very suddenly, with intermittent intervals of unstable high amplitude vibration and clashing. As the velocity was increased slightly, the instability dominated: the vibration amplitude grew rapidly across the entire array and persisted, i.e. the instability was not intermittent. Several modes of vibration were observed, but most apparent was the coupling between the tube columns. The middle (row) tubes seemed to clash with the tubes above and below more frequently than with those in the lateral direction. Each tube appeared to oscillate independent of the others with adjacent tubes moving in and out of phase with one another, indicating different vibration frequencies. Occasionally the dominant transverse oscillation would be replaced with an orbiting motion. The tube motion is much more complex than we anticipated and almost appears to be random with occasional vigorous clashing.

3.2 Normal Triangular Array

The vibration of a sub-group of seven tubes in a normal triangular array was observed over a range of twenty reduced velocities. The configuration of the sub-group of tubes is shown in Fig. 7. The flow is from left to right. These tubes were selected (from the fifteen flexibly mounted tubes in the entire array) for observation because of their representative pattern and symmetrical distribution. Experimental characterization of this sub-group vibration may be comparable to a unit cell in a computational model. The behavior of the larger array of tubes may perhaps be determined by consideration of this sub-group as a basic component, where the geometric pattern of the larger array is formed by spatial extension (e.g. reflection or translation) of the sub-group pattern. Thus, it is of interest to consider such a

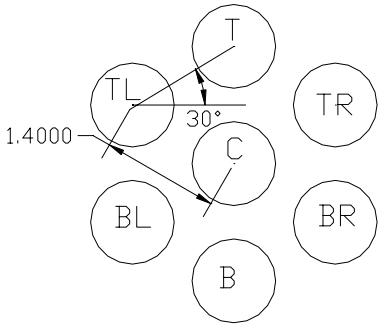

Figure 7. Sub group of normal triangular tube array

"unit" group of tubes.

The exact relationship between the behavior of this sub-group and a larger array of an identical configuration (i.e. a normal triangular array) is yet to be determined. However, it is hoped that observing the dynamics of the vibrations for this group will allow for a basic understanding of the flow-structure interaction and onset of FEI in this configuration.

The displacement of each tube in both the lift and drag directions were measured, as well as the average relative amplitude of vibration over each of the twenty reduced velocities (Fig 8). Several features of the tube array vibration may be noted from the figure. First, at a specific reduced velocity of about 1.4, a sharp increase in the average magnitude of vibration of the tubes occur; as noted before, this feature probably corresponds to vortex shedding. The magnitudes of these vibrations vary greatly from tube to tube in the array; it appears that the two tubes farthest downstream are the most excited, while the top and top left tubes are less than 20% of the average vibration magnitude of downstream tubes. The downstream tubes may be more excited due to the vortices originating from the upstream vibrating tubes. However, until the velocity field of the flow around the flexible tubes is known, the exact reason for this behavior may not be concluded. It is nonetheless useful to know that, in this array configuration, the downstream tubes are indeed more susceptible to vortex-induced vibration.

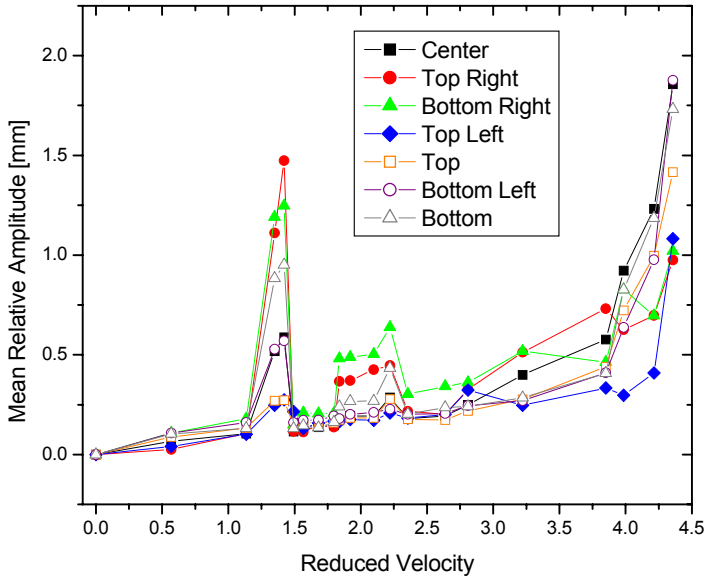

Figure 8. Average Relative Amplitude of Tube Vibration as a function of the Reduced Velocity, Normal Triangular Array Configuration

The maximum displacements associated with the vortex shedding may appear large within the data presented, but are comparatively small in relation to the fluid-elastic instability normally encountered in similar experiments. Furthermore, the vortex-induced vibration mechanism is typically less persistent than FEI, tending to be more intermittent and diminishing quickly when the flow velocity is increased past the region in which the vortex shedding is prevalent. This region may be predicted through calculation of the Strouhal number for the tubes, and thus avoided by proper control of the flow speed. Since the Strouhal number depends only on the structural properties of the tubes and the flow speed, the vortex shedding should occur at exactly the same reduced velocity for a bundle of identical tubes, which is exactly the result reflected by the experimental data.

The second feature to note from the figure is a "step" in the vibration magnitude, starting at a reduced velocity of about 1.8 and culminating with a "spike" at a reduced velocity of about 2.2. The same tubes that were most excited during the vortex shedding are again those that exhibit the largest vibrations. The remaining tubes hardly show any increased response at the "step", but all tubes show some increase at the "spike".

This behavior indicates an excitation mechanism similar to the vortex shedding, an effect related to the overall flow regime and not isolated effects (such as coupling between pairs of tubes). It is suspected that this feature is due to the turbulent transition of the flow around the flexible tubes, causing a change in the distribution of the momentum in the wakes of the tubes. This shift in the wake profiles would induce some force on the tubes, though

perhaps not as strong as the vortex shedding, and would be most evident in the downstream tubes, i.e., the tubes which lie in the wake of the leading tubes.

The onset of FEI appears to occur in an interval of reduced velocity between 3.75 and 4. The behavior of individual tubes vary significantly for reduced velocities greater than 2.8; the vibrations of certain tubes begin to grow even before the onset of FEI, while others change only modestly until instability occurs. Even after the onset, the tubes do not vibrate with equal strength and persistence at a given velocity. While the tubes of the normal triangular array follow a similar trend towards and beyond instability, their individual vibration patterns differ significantly from tube to tube.

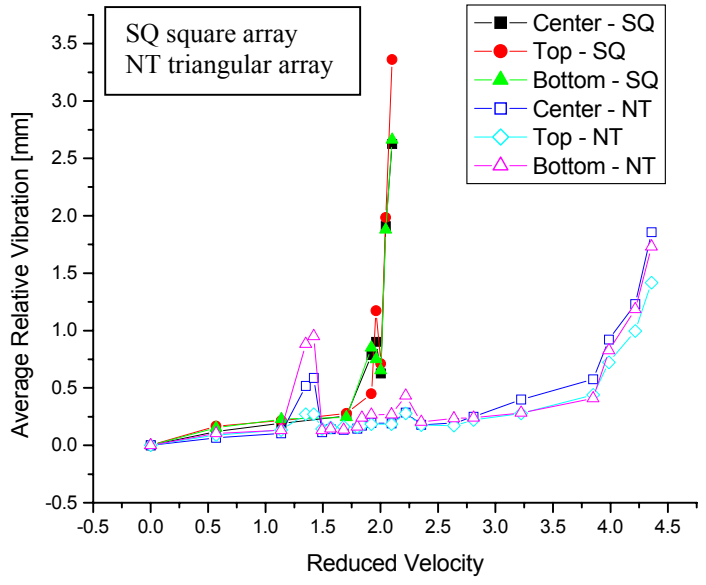

Figure 9. Comparison of FEI onset for the normal triangular array and the square array; SQ denotes square.

Several of the above observations of the normal triangular array vibration may be contrasted with the observations from the vibration of the square tube array. The average relative magnitudes of vibration for three tubes from both the square and the normal triangular array are plotted in figure 9.

In the data from these experiments, both the normal triangular and square tube arrays are of the same diameter (25.4 mm) tubes, pitch-to-diameter ratio (1.4), and natural frequency (16 Hz). The onset of FEI for the normal triangular configuration has been described above; by contrast, the onset of FEI for the square array occurs at a reduced velocity of about 2, whereas the onset for the normal triangular array occurs at twice the flow velocity. Furthermore, the instability of the square array occurs very violently and reaches maximum average vibration magnitudes 50% larger than those attained in the experiments using the triangular array; the instability in the triangular array occurs in a relatively gradual manner, with average vibration magnitudes of less than 2.0mm at flow speeds of over twice those attained in the square array tests.

Another observation of interest is the location at which the vortex shedding occurs for each of the two configurations. The square array exhibits this phenomenon at a reduced velocity nearly coincident with its onset to FEI, whereas the vortex-shedding peak for the triangular array is separated from the onset of FEI by almost 3 units of reduced velocity. Since the reduced velocity depends only on the flow speed (in this case), this separation indicates that the two mechanisms take place under quite different flow regimes; the vortex shedding occurs at a Reynolds number of approximately 12886, while the onset of FEI occurs at Re ~34923. This difference may have some fundamental influence on the manner in which the instability evolves and help explain the differences observed in the FEI between the two configurations. Knowledge of the Reynolds number is not sufficient, however, to determine the nature of the fluid interaction in these two cases; a detailed measurement of the flow speed is again required to support any conclusion regarding the fluid mechanism responsible for the onset of FEI and its influence on the evolution of the instability.

4.0 CONCLUDING REMARKS

A criteria for FEI is somewhat ambiguous because the process is gradual at the initial stages. The amplitude slowly increases as the flow velocity increases and at some point increases very quickly. A stated critical velocity will be a function of what amplitude is chosen. Observations of the tube motion show a very complex pattern emerging. The pattern almost appears to be statistical in nature with the tubes seeming to behave independently of one another. Further the vibration amplitude increases in the flow direction. The reasons for this are complex and demonstrate that one should use data from single oscillating tube experiments with caution.

A square array is far more susceptible to damaging vibration amplitudes than is a triangular array. Further the onset is much more sudden with the vortex shedding instability being a small deviation in the amplitude-velocity relationship. The triangular array response is similar with the velocity scale being stretched and as a result is much less cataclysmic. The velocity where the amplitude begins an exponential growth is nearly three times that of a square array.

Fluid elastic instability is one of the most damaging types of instabilities encountered in heat exchangers and steam generators and can impose a severe economic penalty on the power and chemical industries. At present our understanding of the mechanisms leading to fluid-elastic instability is very limited and more experiments of the type reported here needed to more fully delineate the conditions for the onset of fluid-elastic instability.

ACKNOWLEDGMENTS

The authors gratefully acknowledge the support of NERI program grant Number DE-FG03-00SF22169.

REFERENCES

[1] Blevins, R.D, 1990, *Flow-Induced Vibration, 2nd Edition*, Von Nostrand Reinhold: New York H.

[2] Connors, H. J., Jr., 1970, "Fluidelastic Vibration of Tube Arrays Excited by Cross-Flow," in *Flow Induced Vibration in Heat Exchangers*, ASME Winter Annual Meeting, New York, pp. 42-56T.

[3] Alquadoomi, O., Adinolfi, P., Catton,I., and Dhir, V.K, "*Methods of Analysis of Tube Array Fluid Elastic Instability Data*" to appear in the proceedings of the IMECE, November 2003.

[4] Adinolfi, P. "*Multiple Tube Fluid Elastic Instability Measurment Methods and Experimental Data*", MSc Thesis, UCLA, 2003

[5] Pettigrew, M.J., and Taylor, C.E., 1991, "*Fluidelastic Instability of Heat Exchanger Tube Bundles: Review and Design Recommendations*," ASME J. of Pressure Vessel Technology, **111**, pp. 242-256